

# Discontinuous Hermite Collocation and Diagonally Implicit RK3 for a Brain Tumour Invasion Model

I. E. Athanaskis, M. G. Papadomanolaki, E. P. Papadopoulou and Y. G. Saridakis

**Abstract**—Over the past years mathematical models, based on experimental data from MRI and CT scans, have been well developed to simulate the growth of aggressive forms of malignant brain tumours. The tumour growth model we are considering here, apart from proliferation and diffusion, is being characterized by a discontinuous diffusion coefficient to incorporate the heterogeneity of the brain tissue. For its numerical treatment by high order methods, we have developed a Discontinuous Hermite Collocation (DHC) finite element method, with appropriately discontinuous basis functions associated with the discontinuity nodes, to discretize in space. In this work, together with the classical backward Euler and Crank Nicolson schemes, we also consider the deployment of a third order diagonally-implicit Runge-Kutta (RK3) scheme to discretize in time. Several numerical experiments are included to demonstrate the performance of the method. The numerical investigation conducted, reveals that the DHC-RK3 is an order  $O(\tau^3 + h^4)$  scheme.

**Index Terms**—Gliomas, Discontinuous Hermite Collocation, Backward Euler, Crank Nicolson, Diagonal Implicit Runge-Kutta.

## I. INTRODUCTION

**G**LIOMAS are among the most common and malignant forms of primary brain tumours. The most typical problem in diagnosis and treatment of patients with glioma is the rapid infiltration of tumour cells in adjacent normal tissue. Well known mathematical models, such as [7],[14], [15] and [3], have been developed to simulate the progress of untreated diffusive brain tumours. Their generalization to incorporate the heterogeneity of the brain tissue (white-grey matter) was achieved in the works of Swanson ([11],[12],[13]) by introducing an appropriately discontinuous diffusion coefficient. In such a case the mathematical model is described by ([11]):

$$\frac{\partial \bar{c}}{\partial \bar{t}} = \nabla \cdot (\bar{D}(\bar{\mathbf{x}})\nabla \bar{c}) + \rho \bar{c} \quad (1)$$

where  $\bar{c}(\bar{\mathbf{x}}, \bar{t})$  denotes the tumour cell density,  $\rho$  denotes the net proliferation rate, and  $\bar{D}(\bar{\mathbf{x}})$  is the diffusion coefficient representing the active motility of malignant cells satisfying

$$\bar{D}(\bar{\mathbf{x}}) = \begin{cases} D_g & , \quad \bar{\mathbf{x}} \text{ in Grey Matter} \\ D_w & , \quad \bar{\mathbf{x}} \text{ in White Matter} \end{cases} \quad (2)$$

with  $D_g$  and  $D_w$  scalars and  $D_w > D_g$ , since glioma cells migrate more rapidly in white than in grey matter.

Manuscript received March 18, 2013; revised April 16, 2013.

This work was supported by EU (European Social Fund ESF) and Greek funds through the operational program *Education and Lifelong Learning* of the National Strategic Reference Framework (NSRF) - Research Funding Program: THALIS.

All authors are with the Applied Math & Computers Lab, Department of Sciences, Technical University of Crete, 73100 Chania, Crete, Greece

Email of the corresponding author : yiannis@science.tuc.gr

On the anatomy boundaries zero flux boundary conditions are imposed while for  $\bar{t} = 0$  an initial spatial distribution of malignant cells  $\bar{c}(\bar{\mathbf{x}}, 0) = \bar{f}(\bar{\mathbf{x}})$  is assumed.

The above model has been extensively studied (e.g. [11]-[13]) and found to be effective in simulating the behaviour of real malignant brain tumours in the time frame for gliomas.

Using the dimensionless variables ([11]) :

$$x = \sqrt{\frac{\rho}{D_w}} \bar{x} \quad , \quad t = \rho \bar{t} \quad , \quad c(x, t) = \bar{c} \left( \sqrt{\frac{\rho}{D_w}} \bar{x}, \rho \bar{t} \right) \frac{D_w}{\rho N_0} \quad ,$$

$$\text{and } f(x) = \bar{f} \left( \sqrt{\frac{\rho}{D_w}} \bar{x} \right)$$

with  $N_0 = \int \bar{f}(\bar{x}) d\bar{x}$  to denote the initial number of tumour cells in the brain at  $\bar{t} = 0$ , as well as the transformation

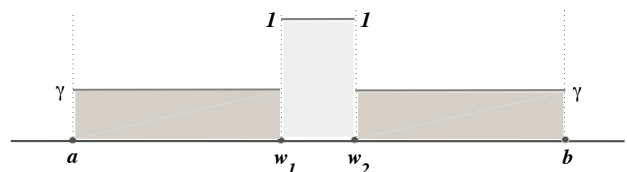
$$c(x, t) = e^t u(x, t) \quad ,$$

the model in 1 + 1 dimensions reduces to

$$\begin{cases} u_t = (Du_x)_x & , \quad x \in [a, b] \quad , \quad t \geq 0 \\ u_x(a, t) = 0 \quad \text{and} \quad u_x(b, t) = 0 & . \\ u(x, 0) = f(x) \end{cases} \quad (3)$$

For the purpose of our analysis, it is enough to consider a multi-domain area consisting of three consecutive regions of grey-white-grey matter. In this case the diffusion coefficient  $D = D(x)$  takes the form

$$D(x) = \begin{cases} \gamma & , \quad a \leq x < w_1 \\ 1 & , \quad w_1 \leq x < w_2 \\ \gamma & , \quad w_2 \leq x \leq b \end{cases} \quad (4)$$



where  $\gamma := \frac{D_g}{D_w} < 1$  is the dimensionless diffusion coefficient in grey matter and 1 is the dimensionless diffusion coefficient in white matter. Furthermore, an initial source of tumour cells  $f(x)$  is considered in the form of

$$f(x) = \sum_{i=1}^K \delta(x - \xi_i) \quad , \quad \xi \in [a, b] \quad , \quad (5)$$

where  $\delta(x)$  denotes Dirac's delta.

Working towards the development of high order numerical schemes, we introduced (cf. [9]) a Collocation method with Hermite cubic elements and appropriate discontinuous nodal basis functions at the interface points to treat the first derivative discontinuities (Section II). In Section III, the Discontinuous Hermite Collocation (DHC) method is coupled with a third order diagonally implicit Runge-Kutta scheme (DIRK) to produce a high order stable method capable of efficiently treating our model problem among many other demanding problems. Its performance is investigated in Section IV through several numerical experiments.

## II. DISCONTINUOUS HERMITE COLLOCATION (DHC)

The discontinuous diffusion coefficient  $D(x)$ , described in (4), directly implies discontinuity of  $u_x$ , hence continuity of  $Du_x$ , across each interface. In fact, as the linear parabolic nature of the initial-boundary value problem (3) implies continuity of  $u$  (or  $c$ ) across each interface, that is

$$[u] := u^+ - u^- = 0 \quad , \quad \text{at } x = w_k \quad , \quad k = 1, 2 \quad , \quad (6)$$

where

$$u^+ := \lim_{x \rightarrow w_k^+} u(x) \quad \text{and} \quad u^- := \lim_{x \rightarrow w_k^-} u(x) \quad ,$$

integration of the equation in (3) over the discontinuity interfaces yields

$$[Du_x] := D^+u_x^+ - D^-u_x^- = 0 \quad , \quad \text{at } x = w_k \quad , \quad k = 1, 2 \quad . \quad (7)$$

Taking into consideration the above continuity constrains an alternative way to state the model can be described by

$$\begin{cases} u_t = Du_{xx} \quad , \quad x \in \mathcal{R}_\ell \quad , \quad \ell = 1, 2, 3 \quad , \quad t \geq 0 \\ u_x(a, t) = 0 \quad \text{and} \quad u_x(b, t) = 0 \\ [u] = 0 \quad \text{and} \quad [Du_x] = 0 \quad \text{at } x = w_k \quad , \quad k = 1, 2 \\ u(x, 0) = f(x) \end{cases} \quad (8)$$

where  $\mathcal{R}_\ell$  define the three regions

$$\mathcal{R}_1 := [a, w_1] \quad , \quad \mathcal{R}_2 := (w_1, w_2) \quad , \quad \mathcal{R}_3 := (w_2, b] \quad . \quad (9)$$

For each region  $t \times \bar{\mathcal{R}}_\ell$  we consider a rectilinear grid with sides parallel to the  $x$  and  $t$  axes. In  $x$ -direction the grid spacing  $h_\ell$  is given by the form

$$\begin{cases} h_1 := (w_1 - a)/N_1 \quad , \\ h_2 := (w_2 - w_1)/N_2 \quad , \\ h_3 := (b - w_2)/N_3 \quad , \end{cases} \quad (10)$$

where  $N_\ell$  denotes the number of subintervals of  $\bar{\mathcal{R}}_\ell$ , and in  $t$ -direction the grid spacing is  $\tau$ .

Then, the grid points  $(x_j, t_n)$  are given by

$$x_j := a + jh \quad , \quad j = 1, \dots, N + 1 \quad , \quad (11)$$

and

$$t_n = n\tau \quad , \quad n = 0, 1, \dots \quad (12)$$

where  $N = N_1 + N_2 + N_3$  and  $h = h_\ell$  when  $x_m \in \bar{\mathcal{R}}_\ell$ .

For sufficiently smooth solutions  $u$ , Hermite cubic polynomial approximations seek fourth order  $O(h_{max}^4)$ ,  $h_{max} = \max\{h_1, h_2, h_3\}$ , approximate solutions  $U(x, t)$  in the form

$$U(x, t) = \sum_{j=1}^{N+1} [\alpha_{2j-1}(t)\phi_{2j-1}(x) + \alpha_{2j}(t)\phi_{2j}(x)] \quad (13)$$

where the *Hermite cubic basis functions*  $\phi_{2j-1}(x)$  and  $\phi_{2j}(x)$ , centered at the node  $x_j$ , are defined by

$$\phi_{2j-1}(x) = \begin{cases} \phi\left(\frac{x_j-x}{h}\right) \quad , \quad x \in I_{j-1} \\ \phi\left(\frac{x-x_j}{h}\right) \quad , \quad x \in I_j \\ 0 \quad , \quad \text{otherwise} \end{cases} \quad , \quad (14)$$

$$\phi_{2j}(x) = \begin{cases} -h\psi\left(\frac{x_j-x}{h}\right) \quad , \quad x \in I_{j-1} \\ h\psi\left(\frac{x-x_j}{h}\right) \quad , \quad x \in I_j \\ 0 \quad , \quad \text{otherwise} \end{cases} \quad (15)$$

with  $I_j := [x_j, x_{j+1}]$ , and the functions  $\phi(s)$  and  $\psi(s)$  being the generating Hermite cubics over  $[0, 1]$ ; that is, for  $s \in [0, 1]$ ,

$$\phi(s) = (1-s)^2(1+2s) \quad , \quad \psi(s) = s(1-s)^2 \quad . \quad (16)$$

Of course, the fictitious elements  $I_0$  and  $I_{N+1}$  are omitted.

For the solution  $u$  of our model problem in (8), since there are discontinuities at the interface points  $w_1 \equiv x_{N_1+1}$  and  $w_2 \equiv x_{N_1+N_2+1}$ , it is apparent that we have to force the approximate solution  $U(x, t)$  (13) to satisfy the conditions described in (7); thus, for  $k = 1, 2$ ,

$$[DU_x] := D^+U_x^+ - D^-U_x^- = 0 \quad , \quad \text{at } x = w_k \quad , \quad (17)$$

or, equivalently, after using well known properties of the Hermite cubic functions,

$$\begin{cases} \gamma \phi_{2i}(x_i^-) = \phi_{2i}(x_i^+) \quad , \quad i = N_1 + 1 \quad , \\ \phi_{2i}(x_i^-) = \gamma \phi_{2i}(x_i^+) \quad , \quad i = N_1 + N_2 + 1 \quad . \end{cases} \quad (18)$$

This can be achieved if, instead of the Hermite cubic basis functions in (15), we define the basis functions  $\phi_{2i}(x)$  as follows:

$$\phi_{2i}(x) = \begin{cases} -\frac{h}{\gamma}\psi\left(\frac{x_i-x}{h}\right) \quad , \quad x \in I_{i-1} \\ h\psi\left(\frac{x-x_i}{h}\right) \quad , \quad x \in I_i \quad , \quad i = N_1 + 1 \\ 0 \quad , \quad \text{otherwise} \end{cases} \quad (19)$$

and

$$\phi_{2i}(x) = \begin{cases} -h\psi\left(\frac{x_i-x}{h}\right) \quad , \quad x \in I_{i-1} \\ \frac{h}{\gamma}\psi\left(\frac{x-x_i}{h}\right) \quad , \quad x \in I_i \quad , \quad i = N_1 + N_2 + 1 \\ 0 \quad , \quad \text{otherwise} \end{cases} \quad (20)$$

shown in figures Fig.1, Fig.2 for  $\gamma = 0.3$ .

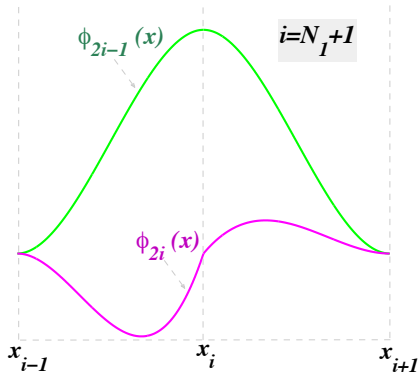


Fig. 1: Cubic basis functions for  $i = N_1 + 1$

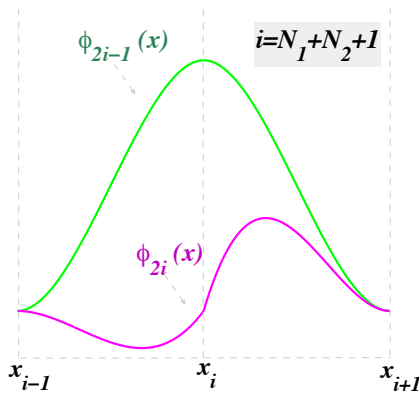


Fig. 2: Cubic basis functions for  $i = N_1 + N_2 + 1$

Substituting the approximate solution (13) in the differential equation we obtain:

$$\sum_{j=1}^{N+1} [\dot{\alpha}_{2j-1}(t)\phi_{2j-1}(x) + \dot{\alpha}_{2j}(t)\phi_{2j}(x)] = D \sum_{j=1}^{N+1} [\alpha_{2j-1}(t)\phi_{2j-1}''(x) + \alpha_{2j}(t)\phi_{2j}''(x)], \quad (21)$$

where the dot defines the first derivative with respect to time. If we now force the above residual to exactly vanish at the two Gaussian collocation points ([2]) in each subinterval and working as in ([9]), the elemental collocation equations that correspond to the element  $I_j$ ,  $j = 1, \dots, N$  take the matrix form:

$$C_j^{(0)} \begin{bmatrix} \dot{\alpha}_{2j-1} \\ \dot{\alpha}_{2j} \\ \dot{\alpha}_{2j+1} \\ \dot{\alpha}_{2j+2} \end{bmatrix} = \frac{D}{h^2} C_j^{(2)} \begin{bmatrix} \alpha_{2j-1} \\ \alpha_{2j} \\ \alpha_{2j+1} \\ \alpha_{2j+2} \end{bmatrix} \quad (22)$$

where  $h$  and  $D$  are as defined in (10) and (4) equations and

$$C_j^{(\kappa)} = \begin{bmatrix} s_1^{(\kappa)} & \frac{h}{\zeta_j} s_2^{(\kappa)} & s_3^{(\kappa)} & -\frac{h}{\beta_j} s_4^{(\kappa)} \\ s_3^{(\kappa)} & \frac{h}{\zeta_j} s_4^{(\kappa)} & s_1^{(\kappa)} & -\frac{h}{\beta_j} s_2^{(\kappa)} \end{bmatrix}, \quad \kappa = 0, 2 \quad (23)$$

with  $s_1^{(0)} = \frac{9+4\sqrt{3}}{18}$ ,  $s_2^{(0)} = \frac{3+\sqrt{3}}{36}$ ,  $s_3^{(0)} = \frac{9-4\sqrt{3}}{18}$ ,  $s_4^{(0)} = \frac{3-\sqrt{3}}{36}$ ,  $s_1^{(2)} = -2\sqrt{3}$ ,  $s_2^{(2)} = -1 - \sqrt{3}$ ,  $s_3^{(2)} = 2\sqrt{3}$  and  $s_4^{(2)} = -1 + \sqrt{3}$ . The constants  $\zeta_j$  and  $\beta_j$  are used to distinguish the elemental matrices for the elements  $I_{N_1}$  and  $I_{N_1+N_2+1}$  since the basis functions in those elements are using equations (20) and (21) respectively. Therefore, for  $j \in \{1, \dots, N\}$

$$\zeta_j = \begin{cases} 1 & , j \neq N_1 + N_2 + 1 \\ \gamma & , j = N_1 + N_2 + 1 \end{cases}, \quad (24)$$

$$\beta_j = \begin{cases} 1 & , j \neq N_1 \\ \gamma & , j = N_1 \end{cases}.$$

To produce the boundary collocation equations we force the approximate solution  $U(x, t)$  to satisfy the boundary conditions at every time step, namely

$$\dot{\alpha}_2 = 0, \quad \alpha_2 = 0, \quad \dot{\alpha}_{2N+2} = 0, \quad \alpha_{2N+2} = 0. \quad (25)$$

A careful assembly of all interior elemental and boundary collocation equations, described above, leads to the system

$$A\dot{\mathbf{a}} = B\mathbf{a} \quad (26)$$

where  $\dot{\mathbf{a}} = [\dot{\alpha}_1 \ \dot{\alpha}_3 \ \dots \ \dot{\alpha}_{2N+1}]^T$ ,  $\mathbf{a} = [\alpha_1 \ \alpha_3 \ \dots \ \alpha_{2N+1}]^T$  and

$$A = \begin{bmatrix} \tilde{A}_1 & B_1 & & & & \\ & A_2 & B_2 & & & \\ & & \backslash & & & \\ & & A_{N-1} & B_{N-1} & & \\ & & & A_N & \tilde{B}_N & \end{bmatrix}, \quad (27)$$

$$B = \begin{bmatrix} \tilde{F}_1 & G_1 & & & & \\ & F_2 & G_2 & & & \\ & & \backslash & & & \\ & & F_{N-1} & G_{N-1} & & \\ & & & F_N & \tilde{G}_N & \end{bmatrix}. \quad (28)$$

with the  $2 \times 2$  matrices  $A_j$ ,  $B_j$ ,  $F_j$  and  $G_j$  are defined through the matrices in (23) and the relationships

$$[A_j \ B_j] = C_j^{(0)} \quad \text{and} \quad [F_j \ G_j] = \frac{D}{h^2} C_j^{(2)}. \quad (29)$$

The tilde analogues of the above matrices are obtained by omitting their second column.

The system (26) can also be written as a system of ODEs in the form:

$$\dot{\mathbf{a}} = C(t, \mathbf{a}) \quad (30)$$

where  $C(t, \mathbf{a}) = A^{-1}B\mathbf{a}$ .

### III. DIAGONALLY IMPLICIT RUNGE-KUTTA SCHEMES

In this section, we couple the DHC method, described in the previous section, with efficient  $A$ -stable diagonally implicit Runge-Kutta (DIRK) schemes. For comparison purposes we also consider the classical backward Euler (BE) and Crank Nicolson (CN) implicit time discretization procedures.

Upon writing the system of ODEs (30) at time level  $t = t_{n+1}$  as

$$\dot{\mathbf{a}}^{(n+1)} = C(t_{n+1}, \mathbf{a}^{(n+1)}) \quad (31)$$

where

$$C(t_{n+1}, \mathbf{a}^{(n+1)}) = A^{-1}B\mathbf{a}^{(n+1)}$$

and

$$\dot{\mathbf{a}}^{(n+1)} = \begin{bmatrix} \dot{\alpha}_1^{(n+1)} & \dot{\alpha}_3^{(n+1)} & \dots & \dot{\alpha}_{2N+1}^{(n+1)} \end{bmatrix}^T$$

$$\mathbf{a}^{(n+1)} = \begin{bmatrix} \alpha_1^{(n+1)} & \alpha_3^{(n+1)} & \dots & \alpha_{2N+1}^{(n+1)} \end{bmatrix}^T ,$$

the classical BE takes the form:

$$\frac{\mathbf{a}^{(n+1)} - \mathbf{a}^{(n)}}{\tau} = C(t_{n+1}, \mathbf{a}^{(n+1)}) \quad (32)$$

or, equivalently,

$$(A - \tau B)\mathbf{a}^{(n+1)} = A\mathbf{a}^{(n)} , \quad (33)$$

where the starting vector  $\mathbf{a}^{(0)}$  is determined in a straight forward way from the model's initial condition (cf. (8) and (5)). Similarly, the CN scheme is expressed as

$$\frac{\mathbf{a}^{(n+1)} - \mathbf{a}^{(n)}}{\tau} = \frac{1}{2}(C(t_{n+1}, \mathbf{a}^{(n+1)}) + C(t_n, \mathbf{a}^{(n)})) \quad (34)$$

or, equivalently,

$$(A - \frac{\tau}{2}B)\mathbf{a}^{(n+1)} = (A + \frac{\tau}{2}B)\mathbf{a}^{(n)} . \quad (35)$$

For an initial value problem in the form  $y_t = g(t, y)$ ,  $y(0) = y_0$ , the well celebrated idea of Runge-Kutta methods (e.g. cf. [4], [5], [1]) is to use weights  $b_i$  and quadrature points  $d_i$ ,  $1 \leq i \leq q$ , to approximate  $y^{(n+1)}$  from  $y^{(n)}$  using the  $q$  intermediate stage formula

$$y^{(n+1)} = y^{(n)} + \tau \sum_{i=1}^q b_i g(t_{n,i}, y^{(n,i)}) , \quad (36)$$

with  $t_{n,i} = t_n + d_i\tau$  and

$$y^{(n,i)} = y^{(n)} + \tau \sum_{j=1}^q a_{ij} g(t_{n,j}, y^{(n,j)}) , \quad 1 \leq i \leq q . \quad (37)$$

Formulas (36) and (37) together define a Runge-Kutta method, which we designate by displaying its coefficients:

$$\begin{array}{ccc|c} a_{11} & \dots & a_{1q} & d_1 \\ \vdots & & \vdots & \vdots \\ a_{q1} & \dots & a_{qq} & d_q \\ \hline b_1 & \dots & b_q & \end{array} \quad (38)$$

The *semi-implicit* (cf. [4], [5]) Runge-Kutta methods, determined by the property  $a_{ij} = 0, j > i$ , and in particular the *diagonally-implicit* (cf. [6], ) Runge-Kutta (DIRK) methods, by further imposing  $a_{ii} = a, i = 1(1)q$ , are the targeted subcategories we are interested in this work. Following the work in [6] (see also [1]) it is well known that, for  $q = 2$ , there is exactly one  $A$ -stable DIRK method of order  $p = 3$  described by:

$$\begin{array}{ccc|c} \lambda & 0 & \lambda & \\ \hline 1 - 2\lambda & \lambda & 1 - \lambda & \\ \hline \frac{1}{2} & \frac{1}{2} & & \end{array} \quad (39)$$

where  $\lambda = \frac{1}{2} + \frac{\sqrt{3}}{6}$ .

Deploying now the (2,3)-DIRK scheme, described above, for the solution of the DHC system of ODE's in (30) we obtain:

$$\mathbf{a}^{(n,1)} = \mathbf{a}^{(n)} + \tau \lambda C(t_{n,1}, \mathbf{a}^{(n,1)})$$

$$\mathbf{a}^{(n,2)} = \mathbf{a}^{(n)} + \tau \left[ (1 - 2\lambda)C(t_{n,1}, \mathbf{a}^{(n,1)}) + \lambda C(t_{n,2}, \mathbf{a}^{(n,2)}) \right]$$

$$\mathbf{a}^{(n+1)} = \mathbf{a}^{(n)} + \frac{\tau}{2} \left[ C(t_{n,1}, \mathbf{a}^{(n,1)}) + C(t_{n,2}, \mathbf{a}^{(n,2)}) \right] \quad (40)$$

or, equivalently,

$$(A - \tau\lambda B)\mathbf{a}^{(n,1)} = A\mathbf{a}^{(n)}$$

$$(A - \tau\lambda B)\mathbf{a}^{(n,2)} = A\mathbf{a}^{(n)} + \tau(1 - 2\lambda)B\mathbf{a}^{(n,1)} . \quad (41)$$

$$A\mathbf{a}^{(n+1)} = A\mathbf{a}^{(n)} + \frac{\tau}{2} [B\mathbf{a}^{(n,1)} + B\mathbf{a}^{(n,2)}]$$

#### IV. NUMERICAL RESULTS

In this section, we numerically investigate the performance of the DHC-DIRK method. For comparison purposes, we also include some results from the performance of the DHC method combined with the classical BE and CN schemes.

The numerical experiments include refer to the following three model problems:

##### Model Problem 1

$$a = -5, w_1 = -1, w_2 = 1, b = 5, \gamma = 0.5$$

and

$$f(x) = \frac{1}{\eta\sqrt{\pi}} e^{-x^2/\eta^2} ,$$

##### Model Problem 2

$$a = -5, w_1 = 1, w_2 = 1.5, b = 5, \gamma = 0.5$$

and

$$f(x) = \frac{1}{\eta\sqrt{\pi}} (e^{-(x+3.5)^2/\eta^2} + e^{-(x-3)^2/\eta^2}) ,$$

##### Model Problem 3

$$a = -5, w_1 = -2, w_2 = 1, b = 5, \gamma = 0.5$$

and

$$f(x) = \frac{1}{\eta\sqrt{\pi}} (e^{-(x-3)^2/\eta^2} + e^{-(x-4)^2/\eta^2}) .$$

In all model problems  $\eta = 0.2$ .

Using the DHC-DIRK method, the tumour growth pattern associated with each one of the above three model problems is depicted in Fig. (3), Fig. (4) and Fig. (5) respectively.

The order of convergence of the DHC, coupled with all time discretization schemes considered here, is show schematically in Fig. (6), Fig. (7) and Fig. (8) for the Model Problems (MP) 1, 2 and 3 respectively. It is apparent that the order of convergence remains four as in the continuous Hermite Collocation.

The order of convergence of all Time Discretization Schemes (TDS) is demonstrated through in Fig. (9), Fig. (10) and Fig. (11) for the Model Problems (MP) 1, 2 and 3 respectively. In all model problems,  $N_t$  denotes the number of time steps and the order of convergence remains one,

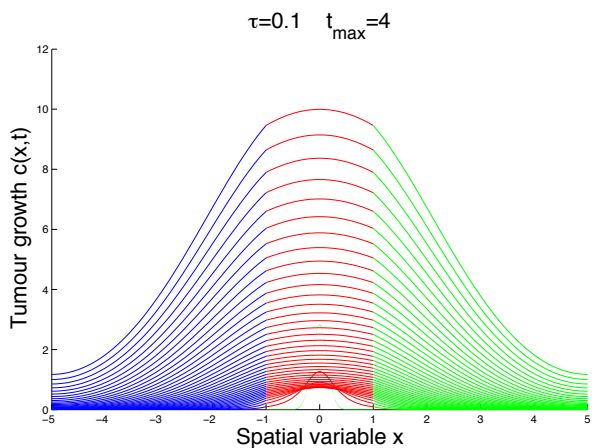


Fig. 3: The behaviour of the method DHC/ DIRK for MP 1

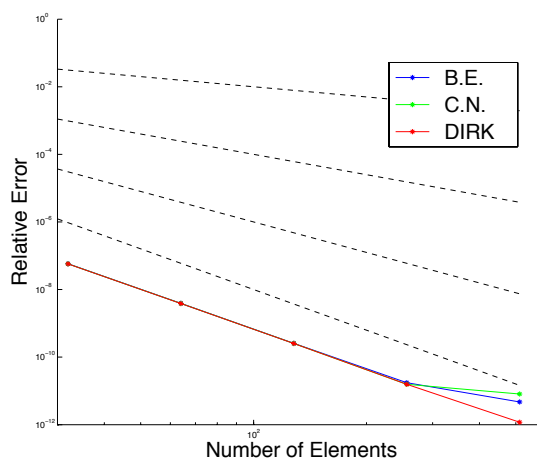


Fig. 6: Order of convergence of the DHC method for MP 1

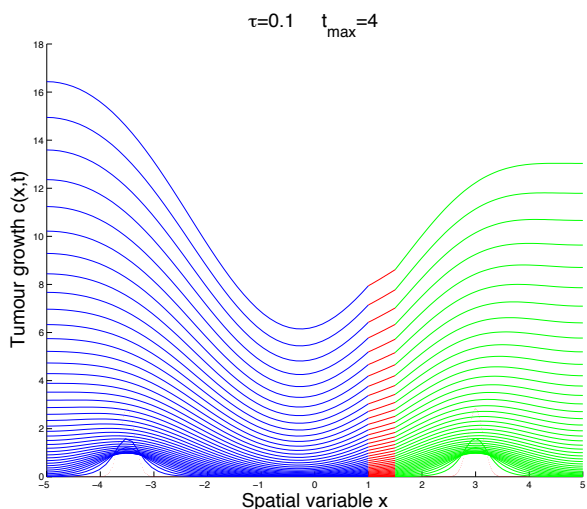


Fig. 4: The behaviour of the method DHC/ DIRK for MP 2

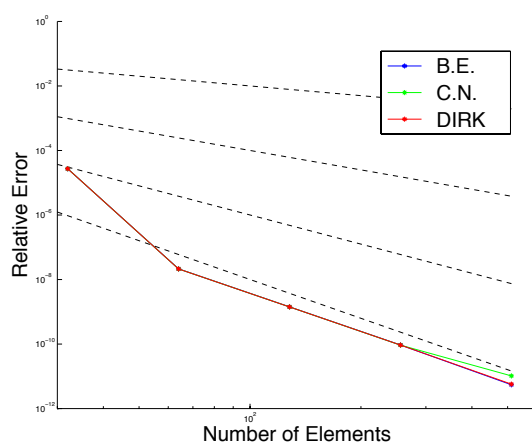


Fig. 7: Order of convergence of the DHC method for MP 2

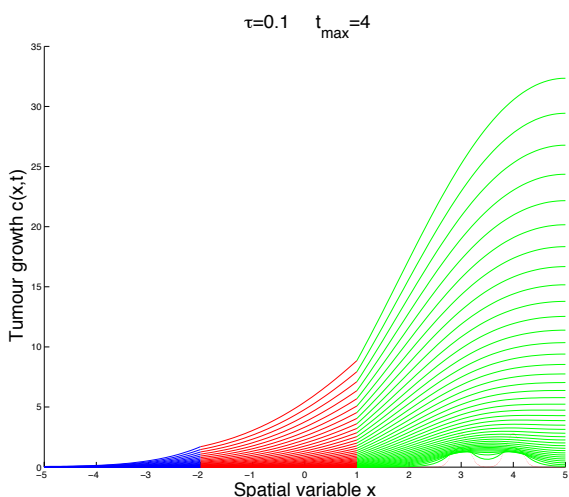


Fig. 5: The behaviour of the method (DHC)/(DIRK) for the model problem 3.

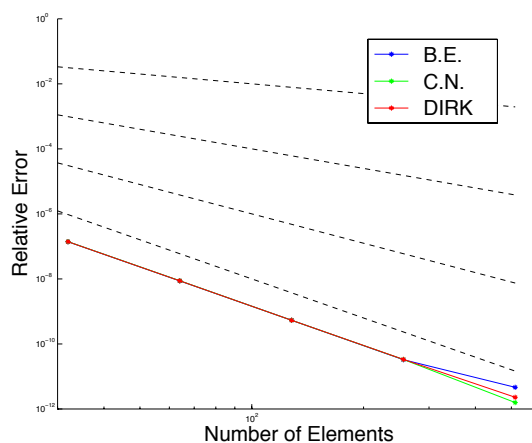


Fig. 8: Order of convergence of the DHC method for MP 3

two and three for BE, CN and DIRK methods, respectively. Observe the behaviour of the CN method due to oscillations at the beginning of the process.

Finally, we include tables Tables I, II and III for the

comparison of all time discretization schemes, coupled with the DHC method, with respect to the computational cost (measured in secs) needed to evolve from  $t = 0$  to  $t = 4$ , using a time step  $\tau = 0.1$ .

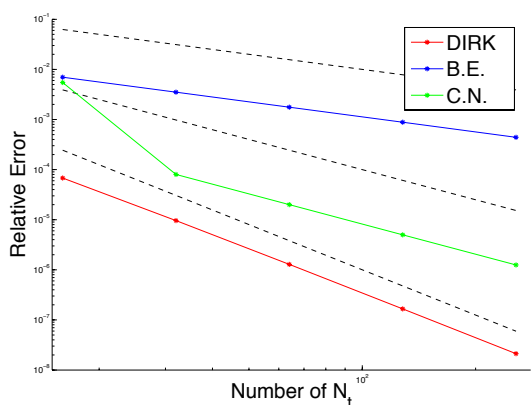


Fig. 9: Order of convergence of the TDS for MP 1

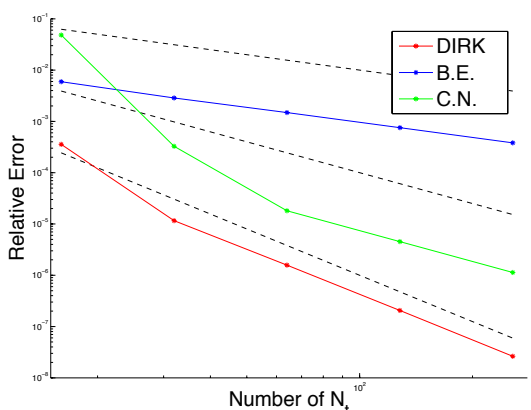


Fig. 10: Order of convergence of the TDS for MP 2

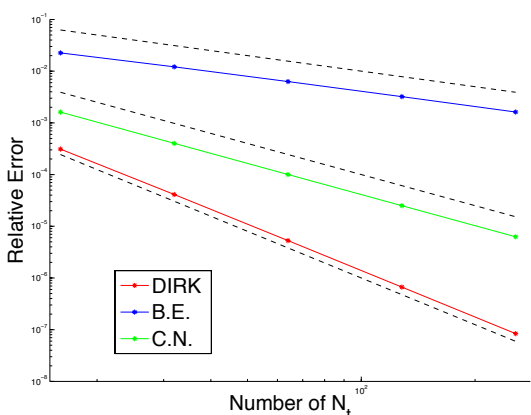


Fig. 11: Order of convergence of the TDS for MP 3

Table I Computational time for MP 1

N	B.E.	C.N.	DIRK
64	0.2445	0.2481	0.2886
128	0.2692	0.2700	0.2797
256	0.3159	0.3193	0.3317
512	0.4050	0.4128	0.4359

Table II Computational time for MP 2

N	B.E.	C.N.	DIRK
64	0.2504	0.2492	0.2560
128	0.2689	0.2756	0.2804
256	0.3170	0.3242	0.3283
512	0.4111	0.4199	0.4269

Table III Computational time for MP 3

N	B.E.	C.N.	DIRK
64	0.2447	0.2520	0.2549
128	0.2694	0.2736	0.2820
256	0.3174	0.3215	0.3328
512	0.4105	0.4248	0.4278

## V. CONCLUSION

In this work, we have investigated the performance of a stable high order method, obtained from the coupling of a fourth order Discontinuous Hermite Collocation method with a third order Diagonally-implicit Runge-Kutta scheme, to treat a brain tumour growth model which, apart from proliferation and diffusion, is being characterized by a discontinuous diffusion coefficient to incorporate the heterogeneity of the brain tissue.

## ACKNOWLEDGMENT

The present research work has been co-financed by the European Union (European Social Fund ESF) and Greek national funds through the Operational Program Education and Lifelong Learning of the National Strategic Reference Framework (NSRF) - Research Funding Program: THALIS. Investing in knowledge society through the European Social Fund.

## REFERENCES

- [1] R. Alexander "Diagonally Implicit Runge-Kutta Methods for stiff ODE's", *SIAM Num. Anal.*, vol. 14, no. 6, pp. 1006-1021, 1977.
- [2] C. de Boor and B. Swartz "Collocation at Gaussian points", *SIAM Num. Anal.*, vol.10, pp. 582-606, 1973.
- [3] P.K. Burgess, P.M. Kulesa, J.D. Murray and E.C. Alvord Jr. "The interaction of growth rates and diffusion coefficients in a three-dimensional mathematical model of gliomas", *Journal of Neuropathology and Experimental Neurology*, vol.56, no. 6, pp.704-713, 1997.
- [4] J.C. Butcher "Implicit Runge-Kutta processes", *Math.Comp.*, vol.18, pp.50-64, 1964.
- [5] J.C. Butcher "The numerical analysis of ordinary differential equations", *John Wiley*, 1987.
- [6] M. Crouzeix "Sur l'approximation des equations differentielles operationnelles lineaires par des methodes de Runge Kutta", *PhD Thesis*, University Paris VI, Paris, 1975.
- [7] G.C. Cruywagen, D.E. Woodward, P. Tracqui, G.T. Bartoo, J.D. Murray and E.C. Alvord Jr. "The modeling of diffusive tumours", *Journal of Biological Systems*, vol.3, pp.937-945, 1995.
- [8] A. R. Mitchell, D.F. Griffiths "The Finite Difference Method in Partial Differential Equations", *John Willey & Sons*, 1980.
- [9] M.G. Papadomanolaki "The collocation method for parabolic differential equations with discontinuous diffusion coefficient: in the direction of brain tumour simulations", *PhD Thesis*, Technical University of Crete, 2012 (in Greek)
- [10] G.D. Smith "Numerical solution of partial equations: finite difference methods (third edition)", *Oxford University Press*, 1985.
- [11] K.R. Swanson "Mathematical modelling of the growth and control of tumour", *PhD Thesis*, University of Washington, 1999.
- [12] K.R. Swanson, E.C. Alvord Jr and J.D. Murray "A quantitative model for differential motility of gliomas in grey and white matter", *Cell Proliferation*, vol.33, pp.317-329, 2000.
- [13] K.R. Swanson, C. Bridge, J.D. Murray and E.C. Alvord Jr "Virtual and real brain tumours: using mathematical modeling to quantify glioma growth and invasion", *J. Neurol. Sci.*, vol.216, pp.1-10, 2003.
- [14] P. Tracqui, G.C. Cruywagen, D.E. Woodward, T. Bartoo, J.D. Murray and E.C. Alvord Jr. "A mathematical model of glioma growth: The effect of chemotherapy on spatio-temporal growth", *Cell Proliferation*, vol.28, pp.17-31, 1995.
- [15] D.E. Woodward, J. Cook, P. Tracqui, G.C. Cruywagen, J.D. Murray, and E.C. Alvord Jr. "A mathematical model of glioma growth: the effect of extent of surgical resection", *Cell Proliferation*, vol.29, pp.269-288, 1996.